



## CLINICAL INVESTIGATIVE STUDY

# Improved detection of multiple sclerosis lesions with T2-prepared double inversion recovery at 3T

Mauro Costagli<sup>1,2</sup>  | Caterina Lapucci<sup>1,3</sup>  | Domenico Zacà<sup>4</sup> | Nicolò Bruschi<sup>1</sup>  |  
 Simona Schiavi<sup>1</sup>  | Lucio Castellan<sup>3</sup>  | Alto Stemmer<sup>5</sup> | Luca Roccatagliata<sup>3,6</sup>  |  
 Matilde Inglese<sup>1,3</sup> 

<sup>1</sup>Department of Neuroscience, Rehabilitation, Ophthalmology, Genetics, Maternal and Child Sciences (DINOEMI), University of Genoa, Genoa, Italy

<sup>2</sup>Laboratory of Medical Physics and Magnetic Resonance, IRCCS Stella Maris, Pisa, Italy

<sup>3</sup>IRCCS Ospedale Policlinico San Martino, Genoa, Italy

<sup>4</sup>Siemens Healthcare, Milano, Italy

<sup>5</sup>Siemens Healthcare, Erlangen, Germany

<sup>6</sup>Department of Health Sciences (DISSAL), University of Genoa, Genoa, Italy

## Correspondence

Matilde Inglese, Clinica Neurologica, Università di Genova, Largo Paolo Daneo 3, 16132 Genoa, Italy.  
 Email: [m.inglese@unige.it](mailto:m.inglese@unige.it)

## Funding information

Italian Ministry of University and Research: DINOEMI Department of Excellence of MIUR 2018–2022 legge 232 del 2016

## Abstract

**Background and Purpose:** Double inversion recovery (DIR) imaging is used in multiple sclerosis (MS) clinical protocols to improve the detection of cortical and juxtacortical gray matter lesions by nulling confounding signals originating from the cerebrospinal fluid and white matter. Achieving a high isotropic spatial resolution, to depict the neocortex and its typically small lesions, is challenged by the reduced signal-to-noise ratio (SNR) determined by multiple tissue signal nulling. Here, we evaluate both conventional and optimized DIR implementations to improve tissue contrast (TC), SNR, and MS lesion conspicuity.

**Methods:** DIR images were obtained from MS patients and healthy controls using both conventional and prototype implementations featuring a T2-preparation module (T2P), to improve SNR and TC, as well as an image reconstruction routine with iterative denoising (ID). We obtained quantitative measures of SNR and TC, and evaluated the visibility of MS cortical, cervical cord, and optic nerve lesions in the different DIR images.

**Results:** DIR implementations adopting T2P and ID enabled improving the SNR and TC of conventional DIR. In MS patients, 34% of cortical, optic nerve, and cervical cord lesions were visible only in DIR images acquired with T2P, and not in conventional DIR images. In the studied cases, image reconstruction with ID did not improve lesion conspicuity.

**Conclusions:** DIR with T2P should be preferred to conventional DIR imaging in protocols studying MS patients, as it improves SNR and TC and determines an improvement in cortical, optic nerve, and cervical cord lesion conspicuity.

## KEYWORDS

cervical cord, gray matter, magnetic resonance imaging, multiple sclerosis, optic nerve

## INTRODUCTION

Inversion recovery is a well-established magnetic resonance imaging (MRI) technique that allows the suppression of undesired signals originating from a tissue of choice. This is achieved by playing the exci-

tation pulse at an appropriate time after a  $\pi$  (180°) inversion pulse: for example, in neuroimaging studies, this strategy can enable suppression of fat, cerebrospinal fluid (CSF), white matter, and specific tissue interfaces.<sup>1–5</sup> Similarly, double inversion recovery (DIR) imaging uses two inversion pulses with appropriate inversion times T11 and T12 to

This is an open access article under the terms of the [Creative Commons Attribution-NonCommercial-NoDerivs](https://creativecommons.org/licenses/by-nc-nd/4.0/) License, which permits use and distribution in any medium, provided the original work is properly cited, the use is non-commercial and no modifications or adaptations are made.

© 2021 The Authors. *Journal of Neuroimaging* published by Wiley Periodicals LLC on behalf of American Society of Neuroimaging.



null the signal of two tissues of choice.<sup>6</sup> DIR has several clinical applications in brain imaging,<sup>7</sup> especially in the study of the cortical gray matter (GM), whose signal can be isolated by nulling the MR signal originating from the white matter (WM) and CSF.<sup>8</sup> DIR has become the technique of choice for the depiction of cortical GM lesions in multiple sclerosis (MS).<sup>9–11</sup> In this scenario, it is necessary to achieve a sufficiently high isotropic spatial resolution, to depict the thin, convoluted structure of the neocortex and its typically small lesions, which is challenged by the reduced signal-to-noise ratio (SNR) determined by multiple tissue signal nulling. These requirements of spatial resolution isotropy and SNR can be achieved with 3-dimensional acquisition schemes,<sup>8</sup> preferably taking advantage of MR scanners operating at high static magnetic field.<sup>12,13</sup>

Being MS lesions best identified on the basis of their long T2 relaxation time,<sup>14</sup> detrimental T1 weighting contamination in DIR image contrast should be minimized. This operation becomes critical at high field, where the T1 relaxation times are longer<sup>15</sup>; hence, for a given time of repetition TR, undesired increased T1 weighting and a lesser recovery of longitudinal magnetization of the tissues of interest hamper lesion conspicuity. One strategy to reduce unwanted T1 weighting is to include a T2-preparation (T2P) module before inversion<sup>16</sup>: such a module employs a  $\pi/2$  (90°) excitation pulse, followed by a series of  $\pi$  refocusing pulses and one final  $-\pi/2$  flip-back pulse. The duration of the T2P module is determined by the interval between the  $\pi/2$  and  $-\pi/2$  pulses, and is chosen such that the transversal magnetization of GM and WM significantly decays during this time, while that of CSF with long T2-time is virtually unaffected and flipped-back at the end of the module. This way, after the first DIR inversion pulse, the GM and WM experience a saturation recovery as their magnetization is close to zero, while the CSF experiences an inversion recovery as in conventional DIR, in the absence T2P module. As a result, a larger signal in the tissues of interest is obtained, with lesser undesired T1 weighting.<sup>3</sup>

Besides the amount of SNR increase that can be achieved with T2P during acquisition, further SNR improvement can be obtained during image reconstruction. In this respect, a promising iterative denoising (ID) approach has been proposed, to enable the reduction of spatially varying noise.<sup>17</sup> This ID technique has recently been included in the reconstruction pipeline of highly accelerated 3-dimensional fluid-attenuated inversion recovery (FLAIR) imaging with otherwise deteriorated quality, and it enabled to recover the detail of unaccelerated acquisitions.<sup>18</sup>

In this study, we evaluated an optimized 3-dimensional DIR prototype implementation featuring a T2P module and image reconstruction with ID, and assessed its performance in detecting cortical, optic nerve, and cervical cord MS lesions.

## METHODS

Twenty-one subjects participated to this study: 18 patients with MS (age:  $40.2 \pm 3.7$  years; 11 with relapsing-remitting MS, 1 with primary progressive MS, 6 with secondary progressive MS; 13 females; disease duration:  $8.2 \pm 2.5$  years) and 3 healthy controls. Data were acquired

**TABLE 1** MPRAGE sequence parameters

Geometry	Sagittal, Phase encoding A >> P
Time of repetition	2300 ms
Time of echo	2.96 ms
Flip angle	8 degrees
Time of inversion	919 ms
Receiver bandwidth	240 Hz/pixel
Parallel imaging	2, GRAPPA
Coverage	256 mm (I >> S) × 240 mm (A >> P) × 208 mm (R >> L)
Acquisition matrix	256 × 240 × 208
Spatial resolution	1 × 1 × 1 mm <sup>3</sup>
Number of averages	1
Time of acquisition (minutes)	5:09

Abbreviations: A >> P, anterior-to-posterior direction; I >> S, inferior-to-superior direction; R >> L, right-to-left direction; GRAPPA, GeneRalized Autocalibrating Partial Parallel Acquisition; MPRAGE, 3-dimensional magnetization-prepared rapid acquisition with gradient echo.

on a 3T MAGNETOM Prisma scanner (Siemens Healthcare, Erlangen, Germany) equipped with a 64-channel head-and-neck coil. The imaging protocol included one T1-weighted 3-dimensional magnetization-prepared rapid acquisition with gradient echo (MPRAGE)<sup>19</sup> with imaging parameters summarized in Table 1, and two types of DIR acquisitions, both based on a prototype 3-dimensional turbo spin echo sequence using variable refocusing pulses<sup>20</sup>: one with T2P<sup>3,16</sup> and one without, with parameters shown in Table 2. Each acquired dataset was reconstructed twice: with and without an ID algorithm<sup>17</sup> integrated directly in the scanner reconstruction pipeline.<sup>18</sup> Therefore, the following four DIR images were obtained:

- DIR, that is, the conventional DIR implementation without T2P and no ID;
- DIR+ID, that is, conventional DIR acquisition followed by image reconstruction using ID;
- T2PDIR, that is, DIR acquired with T2P module;
- T2PDIR+ID, that is, DIR acquired with T2P module, reconstructed with ID.

The datasets above were acquired twice in three healthy controls, with identical parameters, for SNR assessment, as described in detail below. In healthy controls, binary masks representing the GM, WM, and CSF were obtained from the MPRAGE images by using FAST–FMRIB’s Automated Segmentation Tool<sup>21</sup> and were co-registered to the 3-dimensional DIR images with FLIRT–FMRIB’s Linear Image Registration Tool<sup>22</sup>; SNR values in the relevant nonsuppressed tissue (ie, in the GM) were obtained for each type of DIR images and each subject, as follows<sup>23,24</sup>:

$$\text{SNR}_{\text{GM}} = \frac{\text{mean}(S_1 + S_2)|_{\text{GM}}}{\sqrt{2} \text{std}(S_1 - S_2)|_{\text{GM}}}, \quad (1)$$

**TABLE 2** Double inversion recovery (DIR) sequence parameters

Imaging parameters, common to all DIR acquisitions:	
Geometry	Sagittal, Phase encoding A >> P
Time of repetition	5500 ms
Time of echo	270 ms
Turbo factor	173
Times of inversion	2500 and 450 ms
Receiver bandwidth	668 Hz/pixel
Parallel imaging	3 × 2, CAIPIRINHA
Coverage	230 mm (I >> S) × 240 mm (A >> P) × 173 mm (R >> L)
Acquisition matrix	192 × 200 × 144
Spatial resolution	1.2 × 1.2 × 1.2 mm <sup>3</sup>
Number of averages	2
Time of acquisition (minutes)	4:41
T2-preparation module parameters:	
T2-preparation duration	125 ms
Number of refocusing pulses	4

Abbreviations: A >> P, anterior-to-posterior direction; CAIPIRINHA, Controlled Aliasing in Parallel Imaging Results in Higher Acceleration; I >> S, inferior-to-superior direction; R >> L, right-to-left direction.

where  $S_1$  and  $S_2$  represent the voxel signal intensities in the two repeated acquisitions, and  $\text{mean}(\cdot)|_{\text{GM}}$  and  $\text{std}(\cdot)|_{\text{GM}}$  indicate the calculations of signal mean and standard deviation, respectively, within the GM mask in each subject. The relative tissue contrast (TC) between GM and WM was also calculated for each type of DIR images in each subject, according to the following formula:

$$\text{TC} = \frac{S_{\text{GM}} - S_{\text{WM}}}{\frac{S_{\text{GM}} + S_{\text{WM}}}{2}}, \quad (2)$$

where  $S_{\text{GM}}$  and  $S_{\text{WM}}$  represent the mean image intensities in the GM and WM masks, respectively.

The images obtained from the MS patients were inspected by three raters with different levels of experience: one senior neuroradiologist (Rater 1, LR) with 15 years of experience, one neurologist (Rater 2, CL) with 5 years of experience in MS, and one resident neurologist (Rater 3, NB) with 2 years training in MS lesion identification. The images were randomly presented to the raters, who received no information regarding the type of DIR image being examined. The raters identified and counted, by consensus, the MS cortical (intracortical, leukocortical, and subpial), cervical cord, and optic nerve lesions in each of the four series, for each patient. Each lesion was given a score between 1 and 3 (1 = possible lesion; 2 = probable lesion; 3 = obvious lesion). The average score across lesions was computed for each of the four types of DIR images. In this computation, undetected lesions that were visible in at least another DIR image were assigned a score of 0.

To assess the reliability of assigned scores, Rater 2 performed a second reading in a scoring session that took place more than 70 days after

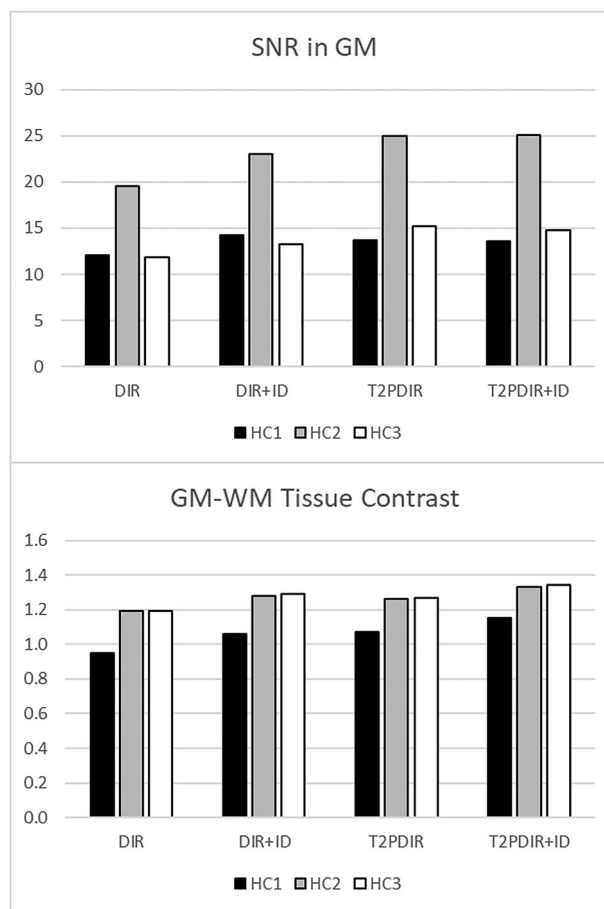


**FIGURE 1** Signal-to-noise ratio (SNR) (top panel) and tissue contrast (bottom panel) in three healthy controls (HC) in conventional double inversion recovery (DIR), DIR reconstructed with iterative denoising (DIR+ID), DIR with T2-preparation module (T2PDIR), and T2PDIR with iterative denoising reconstruction (T2PDIR+ID). GM, gray matter; WM, white matter

the first one. The agreement between the two scoring sessions was measured by the Cohen's  $\kappa$ .<sup>25</sup>

## RESULTS

Figure 1 depicts the SNR in the GM and the GM-WM TC in the four types of DIR images being investigated.

By using T2P, the SNR was improved by 23.3% in the GM on average across subjects, with respect to the conventional DIR acquisition without T2P. ID improved the SNR of conventional DIR by 15.9%, while it did not improve the SNR of T2PDIR: indeed, it reduced it by 1.1%. The joint use of T2P and ID improved the SNR of conventional DIR by 21.9%.

By using T2P, TC was improved by 8.4% on average across subjects, with respect to the conventional DIR acquisition without T2P. ID improved the TC of conventional DIR by 8.9%, while it improved the TC of T2PDIR by 6.6%. The joint use of T2P and ID improved the TC of conventional DIR by 15.5%.

**TABLE 3** List of all detected cortical, optic nerve, and cervical cord multiple sclerosis lesions

Patient	Maximum number of detected lesions	Lesion	Lesion type and location	Score DIR	Score DIR+ID	Score T2PDIR	Score T2PDIR+ID		
1	4	1	IC FRH	2	2	3	3		
		2	LC FLH	2	2	2	2		
		3	CS	3	3	3	3		
		4	CS	1	1	3	1		
2	8	5	IC TLH	3	3	3	3		
		6	LC PLH	1	1	3	3		
		7	LCT LH			3	3		
		8	LC FRH			2	2		
		9	ON			3	3		
		10	CS	2	2	3	3		
		11	CS	1	1	3	3		
		12	CS			1			
3	1	13	IC FLH	2	1				
4	2	14	LCT LH	1	1	1	1		
		15	CS	2	2	2	3		
5	0								
6	9	16	IC OLH	2	2	3	3		
		17	IC TLH			3	3		
		18	LCT LH			3	3		
		19	LC FRH			3	3		
		20	ON			2	2		
		21	CS	1	1	3	3		
		22	CS	1	1	3	3		
		23	CS			3	3		
		24	CS			3	3		
		7	6	25	IC FRH	1	1	3	3
				26	IC PLH			3	2
27	LCT LH					2	2		
28	ON			2	2	3	3		
29	CS			2	3	3	3		
30	CS					2	2		
8	3	31	LC FRH	3	3	3	3		
		32	IC FRH	1	1	2	2		
		33	IC TRH	1	1	2	3		
9	3	34	IC FLH	2	2	2	2		
		35	LCT RH	1	1	2	2		
		36	CS	3	3	3	3		
10	2	37	ON	2	2	3	3		
		38	CS	3	3	3	3		
11	1	39	CS	1	1	1	1		
12	7	40	IC PLH	2	2	2	2		
		41	IC FRH	1	1	1	1		

(Continues)

**TABLE 3** (Continued)

Patient	Maximum number of detected lesions	Lesion	Lesion type and location	Score DIR	Score DIR+ID	Score T2PDIR	Score T2PDIR+ID
		42	ON	2	2	3	3
		43	CS	2	2	3	3
		44	CS	2	2	3	3
		45	CS	2	2	3	3
		46	CS			3	3
13	6	47	LC F LH	2	2	3	3
		48	IC T LH			3	3
		49	LCT RH			3	3
		50	IC T RH			2	2
		51	ON	1	1	3	3
		52	CS	1	2	3	3
14	2	53	LC F RH		1	2	2
		54	ON			3	3
15	4	55	IC T RH	3	3	3	3
		56	LCT RH	2	2	2	3
		57	LCT LH	1	1	1	3
		58	CS	1	2	2	3
16	1	59	ON			1	2
17	2	60	CS			3	3
		61	CS			3	3
18	6	62	ON	1	1	3	3
		63	ON	1	1	3	3
		64	CS	3	3	3	3
		65	CS	1	1	3	3
		66	CS	1	1	3	3
		67	CS	1	1	3	3
Average score:				1.13	1.19	2.62	2.68

*Note:* For each lesion, the table indicates if it is an intracortical (IC), leukocortical (LC), optic nerve (ON), or cervical spine (CS) lesion. For cortical lesions, the lobe (F: frontal; P: parietal; T: temporal; O: occipital) and hemisphere (RH: right hemisphere; LH: left hemisphere) are indicated. For all lesions, the four rightmost columns indicate the scores (1: possible lesion; 2: probable lesion; 3: obvious lesion) assigned in the four types of double inversion recovery (DIR) images: conventional DIR, DIR reconstructed with iterative denoising (DIR+ID), DIR with T2-preparation module (T2PDIR), and T2PDIR with iterative denoising reconstruction (T2PDIR+ID). In the computation of the average scores indicated in the last row of the table, a score of 0 has been assigned to undetected lesions.

In the patients with MS, 15 leukocortical lesions, 15 intracortical lesions, 10 optic nerve lesions, and 27 cervical cord lesions were detected with different levels of confidence, as reported in detail in Table 3. No subpial lesions were detected. Of the 30 cortical lesions, 13 lesions (43%: seven leukocortical and six intracortical lesions) were visible only in DIR images acquired with T2P. Similarly, four out of 10 optic nerve lesions (40%) and six out of 27 cervical cord lesions (22%) were visible only in DIR images acquired with T2P. Only one possible/probable intracortical lesion (Lesion #13 in Table 3) and one possible cervical cord lesion (Lesion #12) were detected only in conventional DIR acquisitions without T2P, and not in DIR acquisitions with T2P (2/67; 3%). Pie charts representing the

improved lesion detection achieved with T2P are shown in Figure 2. The clear improvement in lesion detection obtained with T2P is reflected in the large increase in average scores, indicated at the bottom of Table 3. The average score obtained with T2PDIR (2.62) was 1.49 points higher than that obtained with conventional DIR (1.13). Instead, in the studied cases, image reconstruction with ID did not improve lesion conspicuity. The average scores obtained after ID were only 0.06 points higher than those obtained without ID, both in the comparison between DIR and DIR+ID, and between T2PDIR and T2PDIR+ID.

The total number of cortical, optic nerve, and cervical cord lesions detected in a second, control scoring session was 67, that is, the same

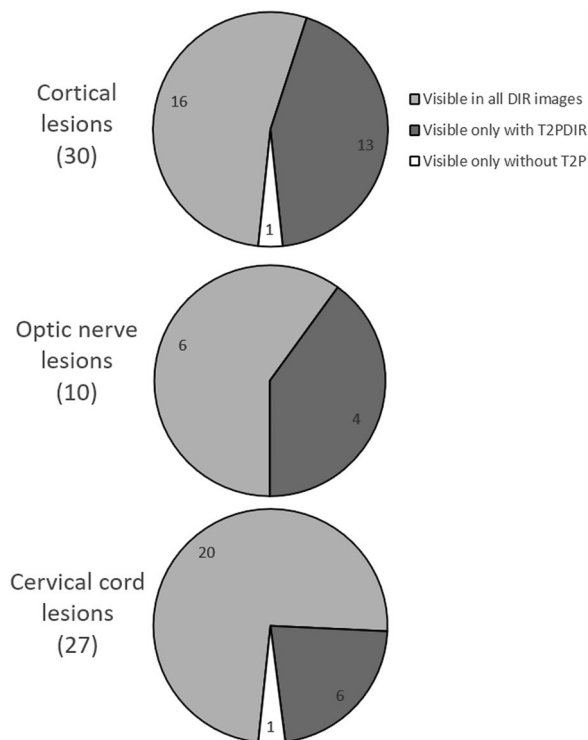


**FIGURE 2** Pie charts indicating the number of lesions detected in the cortical gray matter, optic nerve, and cervical cord, showing in gray the number of lesions detected with both conventional double inversion recovery (DIR) and DIR with T2-preparation module (T2PDIR), in dark gray the lesions visible only in T2PDIR acquisitions, and in white the lesions detected only in conventional DIR acquisition

as in the first session. Intersession scoring reliability was very good, as measured by Cohen's  $\kappa = .97$ .

Figure 3 depicts representative lesions in the different types of DIR images.

## DISCUSSION

The visualization of cortical GM lesions, optic nerve lesions, and cervical cord lesions is typically challenging with conventional T2 and T2-FLAIR imaging.<sup>11</sup> The aim of this study was to assess the improvement obtained by the use of a T2-preparation module and an ID reconstruction routine, applied to a 3-dimensional DIR imaging protocol for detecting small MS lesions, namely, cortical GM lesions, optic nerve lesions, and cervical cord lesions. Our study shows that both T2P and ID improve SNR and TC, and their joint use outperforms the SNR and TC of conventional DIR imaging. From a lesion detection standpoint, a major improvement is achieved by T2P, while ID has a minor impact, at least in the patients studied here. The importance of T2P in improving SNR and TC in the brain was previously demonstrated in studies conducted on MRI scanners operating at ultrahigh field (7T),<sup>26</sup> where the lengthening of GM and WM T1 relaxation time introduces undesired T1 contrast and causes SNR reduction. Our study demonstrated that T2P in 3-dimensional DIR is important not only at 7T, but

also at 3T, as it improves SNR and TC and, most importantly, it determines an improvement in cortical, optic nerve, and cervical cord lesion conspicuity with respect to conventional DIR.

Improving the capability of DIR sequences in revealing cortical lesions, besides providing a more reliable and time-saving approach for neuroimaging examinations, may deeply impact on the MS diagnostic process, as cortical and juxtacortical areas have been already indicated in the current diagnostic criteria to meet dissemination in space (DIS).<sup>27,28</sup> Previous studies demonstrated that the accrual of cortical lesions in patients with MS, especially if treated, is generally very slow over time, also in the progressive forms of the disease.<sup>29,30</sup> Therefore, optimized DIR imaging may reduce the risk of underestimating the cortical lesion burden throughout the course of the disease. Furthermore, it has been demonstrated that the presence of cortical lesions largely contributes to explain disability accrual over time,<sup>31</sup> thus influencing therapeutic choices since the earliest stages of the disease.

In the detection of optic nerve lesions, one major confounder is perineural CSF, whose signal may produce partial volume effects that impair the detection of pathological findings.<sup>32</sup> DIR has been used to study optic nerve pathology,<sup>33-37</sup> with a better representation of lesions than other MR techniques.<sup>7,38</sup> Here, we demonstrated the utility of the T2P module, which further improved optic nerve lesion conspicuity with respect to the conventional DIR implementation, at no cost in terms of additional scanning time. The importance of these findings shall be considered in the light of the fact that optic neuritis is the typical first presentation of the disease (although its inclusion in the DIS criteria for MS is still under debate)<sup>27</sup> and the development of asymptomatic optic nerve lesions is not a rare event in MS.<sup>39</sup>

In the study of spinal cord MS lesions, DIR is not commonly included in MR protocols,<sup>40-42</sup> even though the current guidelines<sup>28</sup> underline the importance of spinal cord examination at disease onset and during monitoring. While, on the one hand, it has been shown that DIR allows better detection of lesions of the cervical segment in comparison with conventional turbo spin echo sequences,<sup>43</sup> on the other hand, proton density-weighted fast spin echo and short tau inversion recovery can detect more lesions compared to DIR.<sup>44</sup> Our results, despite being obtained only in the cervical segment of the spine, demonstrated a clearly better detection of MS lesions by using T2P, which encourages further studies to assess whether T2PDIR, either with or without ID, may be considered for future inclusion in MRI protocols addressing spinal cord lesions in MS.

It is worth noticing two limitations of this study. The first, mentioned previously, is that the evaluation on patients with MS is based on a relatively small number of subjects. However, this number of subjects appears sufficient for the purpose, as it allowed to assess 67 among intracortical, leukocortical, optic nerve, and cervical cord lesions, with at least 10 representative lesions per lesion type. The second limitation is that the results shown here obviously depend on the acquisition parameters adopted in this study. However, the choice of all acquisition parameters was based on well-established criteria<sup>3</sup> and was supported by the published literature on DIR with and without T2P module.<sup>33,37,43</sup>

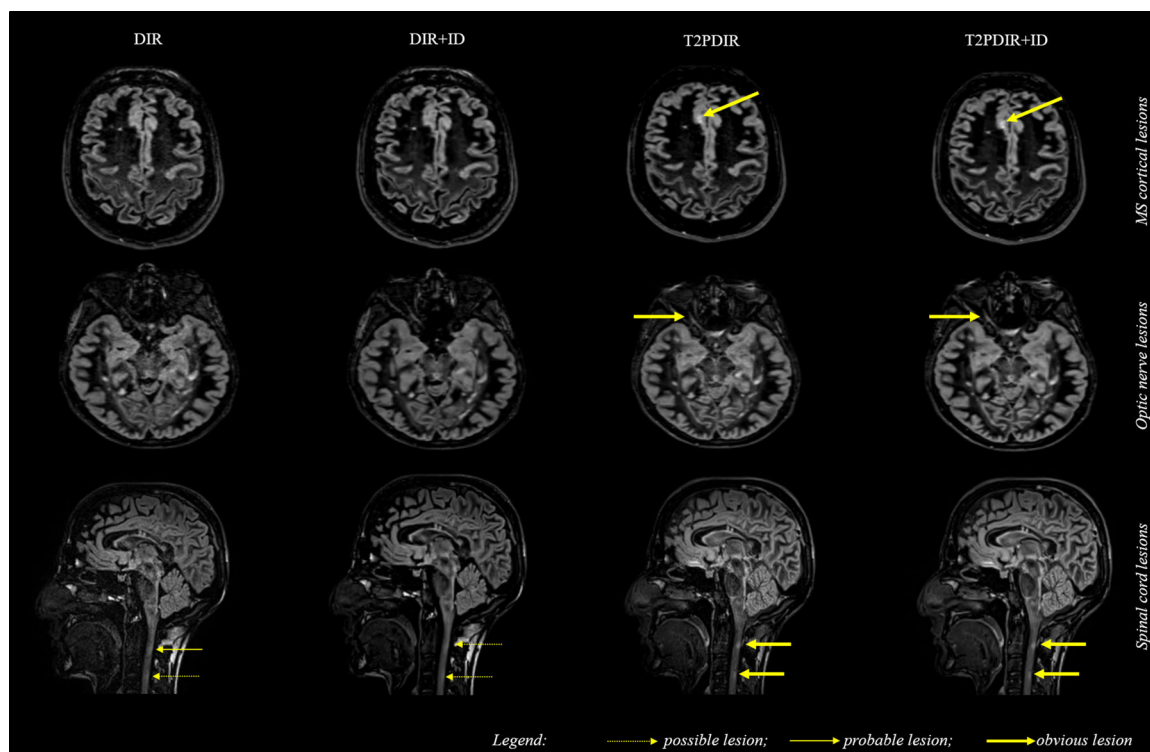


**FIGURE 3** Examples of cortical, optic nerve, and spinal cord lesions, detected with different confidence levels, in conventional double inversion recovery (DIR), DIR reconstructed with iterative denoising (DIR+ID), DIR with T2-preparation module (T2PDIR), and T2PDIR with iterative denoising reconstruction (T2PDIR+ID). Dotted arrows indicate possible lesions (score = 1); thin arrows indicate probable lesions (score = 2); thick arrows indicate obvious lesions (score = 3).

In conclusion, this study demonstrated the clear improvement provided by T2-preparation in 3-dimensional DIR acquisition in the detection of cortical, optic nerve, and cervical cord MS lesions in a clinical 3T MR setting. Therefore, T2PDIR should be preferred to conventional DIR acquisitions in MRI clinical protocols studying MS patients. DIR image reconstruction with ID deserves future investigation: while it has recently been shown that this technique is capable of restoring the quality of highly accelerated acquisitions with otherwise low SNR,<sup>18</sup> ID did not provide obvious further improvements in MS lesion detection in our case of high-quality input images. Further studies shall assess whether ID applied to highly accelerated T2PDIR could enable similar lesion detection performance in a shorter time. In the current state of the art, reconstructing the acquired T2PDIR data both with and without ID appears to be a reasonable approach, which provides two datasets with possibly complementary information.

#### ACKNOWLEDGEMENTS AND DISCLOSURES

The authors would like to acknowledge the work of Dr. Alexis Vaussy (Siemens Healthcare, Saint-Denis, France) in sequence parameter optimization. This work was developed within the framework of the DINOEMI Department of Excellence of MIUR 2018–2022 (legge 232 del 2016).

Domenico Zacà and Alto Stemmer are employees of Siemens Healthcare. Matilde Inglese received fees for participating in advisory boards from Roche, Biogen, Merck, and Genzyme. The other authors declare no conflict of interest.

Open Access Funding provided by Università degli Studi di Genova within the CRUI-CARE Agreement.

#### ORCID

Mauro Costagli [ID](https://orcid.org/0000-0001-9073-1082) <https://orcid.org/0000-0001-9073-1082>  
 Caterina Lapucci [ID](https://orcid.org/0000-0002-3527-6520) <https://orcid.org/0000-0002-3527-6520>  
 Nicolò Bruschi [ID](https://orcid.org/0000-0002-2263-9441) <https://orcid.org/0000-0002-2263-9441>  
 Simona Schiavi [ID](https://orcid.org/0000-0003-1641-186X) <https://orcid.org/0000-0003-1641-186X>  
 Lucio Castellani [ID](https://orcid.org/0000-0002-5463-8785) <https://orcid.org/0000-0002-5463-8785>  
 Luca Roccatagliata [ID](https://orcid.org/0000-0001-8029-3947) <https://orcid.org/0000-0001-8029-3947>  
 Matilde Inglese [ID](https://orcid.org/0000-0002-9610-0297) <https://orcid.org/0000-0002-9610-0297>

#### REFERENCES

- Dwyer AJ, Frank JA, Sank VJ, et al. Short-Ti inversion-recovery pulse sequence: analysis and initial experience in cancer imaging. *Radiology* 1988;168:827-36.
- Hajnal JV, Coene BD, Lewis PD, et al. High signal regions in normal white matter shown by heavily T2-weighted CSF nulled IR sequences. *J Comput Assist Tomogr* 1992;16:506-13.
- Saranathan M, Worters PW, Rettmann DW, et al. Physics for clinicians: fluid-attenuated inversion recovery (FLAIR) and double inversion recovery (DIR) Imaging. *J Magn Reson Imaging* 2017;46:1590-600.
- Tourdias T, Saranathan M, Levesque IR, et al. Visualization of intrathalamic nuclei with optimized white-matter-nulled MPRAGE at 7 T. *Neuroimage* 2014;84:534-45.
- Costagli M, Kelley DAC, Symms MR, et al. Tissue border enhancement by inversion recovery MRI at 7.0 Tesla. *Neuroradiology* 2014;56:517-23



6. Redpath TW, Smith FW. Technical note: use of a double inversion recovery pulse sequence to image selectively grey or white brain matter. *Br J Radiol* 1994;67:1258-63
7. Umino M, Maeda M, li Y, et al. 3D double inversion recovery MR imaging: clinical applications and usefulness in a wide spectrum of central nervous system diseases. *J Neuroradiol* 2019;46:107-16.
8. Boulby PA, Symms MR, Barker GJ. Optimized interleaved whole-brain 3D double inversion recovery (DIR) sequence for imaging the neocortex. *Magn Reson Med* 2004;51:1181-6.
9. Geurts JGG, Pouwels PJW, Uitdehaag BMJ, et al. Intracortical lesions in multiple sclerosis: improved detection with 3D double inversion-recovery MR imaging. *Radiology* 2005;236:254-60.
10. Moraal B, Roosendaal SD, Pouwels PJW, et al. Multi-contrast, isotropic, single-slab 3D MR imaging in multiple sclerosis. *Eur Radiol* 2008;18:2311-20.
11. Geurts JGG, Roosendaal SD, Calabrese M, et al. Consensus recommendations for MS cortical lesion scoring using double inversion recovery MRI. *Neurology* 2011;76:418-24.
12. Balchandani P, Naidich TP. Ultra-high-field MR neuroimaging. *Am J Neuroradiol* 2015;36:1204-15.
13. Inglese M, Fleysher L, Oesingmann N, et al. Clinical applications of ultra-high field magnetic resonance imaging in multiple sclerosis. *Expert Rev Neurother* 2018;18:221-30.
14. Fazekas F, Barkhof F, Filippi M, et al. The contribution of magnetic resonance imaging to the diagnosis of multiple sclerosis. *Neurology* 1999;53:448-56.
15. Rooney WD, Johnson G, Li X, et al. Magnetic field and tissue dependencies of human brain longitudinal 1H<sub>2</sub>O relaxation in vivo. *Magn Reson Med* 2007;57:308-18.
16. Visser F, Zwanenburg JJM, Hoogduin JM, et al. High-resolution magnetization-prepared 3D-FLAIR imaging at 7.0 Tesla. *Magn Reson Med* 2010;64:194-202.
17. Kannengiesser SAR, Mailhe B, Nadar M, et al. Universal iterative denoising of complex-valued volumetric MR image data using supplementary information. Presented at the 24th Annual Meeting of the International Society for Magnetic Resonance in Medicine; May 7-13, 2016; Singapore.
18. Eliezer M, Vaussy A, Toupin S, et al. Iterative denoising accelerated 3D SPACE FLAIR sequence for brain MR imaging at 3T. *Diagn Interv Imaging* 2022;103:13-20.
19. Mugler JP, Brookeman JR. Three-dimensional magnetization-prepared rapid gradient-echo imaging (3D MP RAGE). *Magn Reson Med* 1990;15:152-7.
20. Mugler JP. Optimized three-dimensional fast-spin-echo MRI. *J Magn Reson Imaging* 2014;39:745-67.
21. Zhang Y, Brady M, Smith S. Segmentation of brain MR images through a hidden Markov random field model and the expectation-maximization algorithm. *IEEE Trans Med Imaging* 2001;20:45-57.
22. Jenkinson M, Bannister P, Brady M, et al. Improved optimization for the robust and accurate linear registration and motion correction of brain images. *Neuroimage* 2002;17:825-41.
23. Dietrich O, Raya JG, Reeder SB, et al. Measurement of signal-to-noise ratios in MR images: influence of multichannel coils, parallel imaging, and reconstruction filters. *J Magn Reson Imaging* 2007;26:375-85.
24. Price RR, Axel L, Morgan T, et al. Quality assurance methods and phantoms for magnetic resonance imaging: report of AAPM nuclear magnetic resonance Task Group No. 1. *Med Phys* 1990;17:287-95.
25. Cohen J. A Coefficient of agreement for nominal scales. *Educ Psychol Meas* 1960;20:37-46.
26. De Graaf WL, Zwanenburg JJM, et al. Lesion detection at seven Tesla in multiple sclerosis using magnetisation prepared 3D-FLAIR and 3D-DIR. *Eur Radiol* 2012;22:221-31.
27. Thompson AJ, Banwell BL, Barkhof F, et al. Diagnosis of multiple sclerosis: 2017 revisions of the McDonald criteria. *Lancet Neurol* 2018;17:162-73.
28. Wattjes MP, Ciccarelli O, Reich DS, et al. 2021 MAGNIMS-CMSC-NAIMS consensus recommendations on the use of MRI in patients with multiple sclerosis. *Lancet Neurol* 2021;20:653-70.
29. Calabrese M, Rocca MA, Atzori M, et al. Cortical lesions in primary progressive multiple sclerosis: a 2-year longitudinal MR study. *Neurology* 2009;72:1330-6.
30. Treaba CA, Granberg TE, Sormani MP, et al. Longitudinal characterization of cortical lesion development and evolution in multiple sclerosis with 7.0-T MRI. *Radiology* 2019;291:710-49.
31. Haider L, Prados F, Chung K, et al. Cortical involvement determines impairment 30 years after a clinically isolated syndrome. *Brain* 2021;144:1384-95.
32. Hickman SJ, Miszkiel KA, Plant GT, et al. The optic nerve sheath on MRI in acute optic neuritis. *Neuroradiology* 2005;47:51-55.
33. Hodel J, Outteryck O, Bocher A-L, et al. Comparison of 3D double inversion recovery and 2D STIR FLAIR MR sequences for the imaging of optic neuritis: pilot study. *Eur Radiol* 2014;24:3069-75.
34. Hadhoum N, Hodel J, Defoort-Dhellemmes S, et al. Length of optic nerve double inversion recovery hypersignal is associated with retinal axonal loss. *Mult Scler* 2016;22:649-58.
35. Sartoretti T, Sartoretti E, Rauch S, et al. How common is signal-intensity increase in optic nerve segments on 3D double inversion recovery sequences in visually asymptomatic patients with multiple sclerosis? *Am J Neuroradiol* 2017;38:1748-53.
36. London F, Zéphir H, Hadhoum N, et al. Optic nerve double inversion recovery hypersignal in patients with clinically isolated syndrome is associated with asymptomatic gadolinium-enhanced lesion. *Mult Scler J* 2019;25:1888-95.
37. Riederer I, Mühlau M, Hoshi M-M, et al. Detecting optic nerve lesions in clinically isolated syndrome and multiple sclerosis: double-inversion recovery magnetic resonance imaging in comparison with visually evoked potentials. *J Neurol* 2019;266:148-56.
38. Chow LS, Paley MNJ. Recent advances on optic nerve magnetic resonance imaging and post-processing. *Magn Reson Imaging* 2021;79:76-84.
39. Outteryck O, Lopes R, Drumez É, et al. Optical coherence tomography for detection of asymptomatic optic nerve lesions in clinically isolated syndrome. *Neurology* 2020;95:e733-44.
40. Gass A, Rocca MA, Agosta F, et al. MRI monitoring of pathological changes in the spinal cord in patients with multiple sclerosis. *Lancet Neurol* 2015;14:443-54.
41. Chen Y, Haacke EM, Bernitsas E. Imaging of the spinal cord in multiple sclerosis: past, present, future. *Brain Sci* 2020;10:1-19.
42. Filippi M, Rocca MA, Ciccarelli O, et al. MRI criteria for the diagnosis of multiple sclerosis: MAGNIMS consensus guidelines. *Lancet Neurol* 2016;15:292-303.
43. Riederer I, Karampinos DC, Settles M, et al. Double inversion recovery sequence of the cervical spinal cord in multiple sclerosis and related inflammatory diseases. *AJNR Am J Neuroradiol* 2015;36:219-25.
44. Chang CA, Chong AL, Chandra RV, et al. Detection of multiple sclerosis lesions in the cervical cord: which of the MAGNIMS "mandatory" non-gadolinium enhanced sagittal sequences is optimal at 3T? *Neuroradiol J* 2021;34:600-6.

**How to cite this article:** Costagli M, Lapucci C, Zacà D, Bruschi N, Schiavi S, Castellani L, et al. Improved detection of multiple sclerosis lesions with T2-prepared double inversion recovery at 3T. *J Neuroimaging*. 2022;32:902-909. <https://doi.org/10.1111/jon.13021>